Journal of Simulation and Analysis of Novel Technologies in Mechanical Engineering
16 (2) (2024) 0083~0092
DOI 10.71939/jsme.2024.1130580

Research article

Creep analysis in two functionally graded material rotating gears

Milad Kharati Asl[1], Ali Akbar Lotfi Neyestanak*[2], Saeed Daneshmand[3]

[1, 2]*Department of Engineering, Yadegar-e-Imam Khomeini (RAH), Shahr-e-Rey Branch, Islamic Azad University, Tehran, Iran*
[3]*Department of Mechanical Engineering, Isfahan (Khorasgan) Branch, Islamic Azad University, Isfahan, Iran*

*aklotfi@gmail.com

(Manuscript Received --- 31 Aug. 2024; Revised --- 05 Dec. 2024; Accepted --- 15 Dec. 2024)

Abstract

Spur gears are one of the mechanical structures which widely used in power transmission. They are used to control the speed or change the direction of a power resource. The gears generally fail when creep impacts increases. In practice, most gear teeth break due to surface contact, specially magnifying the high stress concentration on the contact tooth surface. Selecting the suitable material for a gear tooth is of high importance for operating gear system. Utilizing functionally graded material (FGM) can boost up the root strength of tooth and life of the gear manufacturing; therefore, this paper aims to study the effect of functionally graded material layer toward the radial direction in spur gears under in rotating load. Various Young's modulus variation functions and Poisson constant coefficient are used. The subroutine UMAT Abacus has been applied to study the creep behavior in two rotating gears. The effects of material equation and the speed of rotation between gears on the creep behavior have been investigated. According to the results of simulations, the Al–TiB FGM had minimum creep deflection, which was analysis in details with considering the variation of strain, stress and displacement.

Keywords: Spur gears, Functionally graded material, Creep, Stress, Strain.

1- Introduction

Gear is a mechanical element playing a pivotal role in power transmission system. It is widespread component in locomotives, clocks and within all heating industries. Spur gears are one of the most popular types of gears owing to its design simplicity, less maintenance requirement, and economical manufacturing. The gear fails when the applied load exceeds certain limits. Two types of gear tooth failures are common. One of which is breakage of the tooth due to static and dynamic loads. Surface destruction can also result in gear tooth failure; therefore, the gear material should have sufficient strength to avoid failure due to the breakage of the tooth [1, 2]. In most applications utilizing spur gears, they undergo several loading of thermal and mechanical distributions, which cause severe creep deflections shortening the lifetime of spur gears. Magnesium, or aluminum alloys, used to meet demands for reducing the weight of transmission components, is expected to

ensure high durability and corrosion resistance. However, the aluminum and its alloys creep cause considerable obstacles regarding the applications. Various experimental and numerical studies of materials creep have illustrated that the creep deformation of alloys-based Aluminum and Magnesium composite or reinforced with silicon carbide (SiC) ceramic, is less than pure metals by several orders of magnitude. However, the weakness of aluminum is the high thermal expansion coefficient compared to similar metals [3]. Magnesium and Aluminum composites and themes alloys containing SiC ceramic particles can possibly improve the strength and surface hardness. Also, an appropriate choice of geometry and size, the content of the reinforced composites helps to reducing cost with improved efficiency. Mechanical properties including surface hardness and stability of temperature and strength improved by Magnesium and Aluminum alloy-based composites consisting of SiC particles. These composites are suitable for mating gears during rotation involving enhanced temperature [4-6]. In addition, surface roughness playing an essential role in the rotating, this tribology parameter should be decrease. In order to obtain smooth gear surface, selection of Magnesium and Aluminum alloy-based composites could be effeteness. Some engineering applications with high-value surface roughness provide high temperature situation owing to the simultaneous presence of thermal loading and its gradients, where the above-mentioned materials may not be suitable. Obviously, the appeared temperature gradient effects on the gears life. Thus, the idea of functionally graded materials (FGMs) originated and provides the progressive in the field of heat resistant materials. Proposed Materials (FGMs) are particular types of composites with the inhomogeneous pattern of constituent's distribution. Constituent's distribution depended on the applications. On the higher-temperature part usually, used the heat-resistant ceramics and on another lower-temperature part applied the hard metals with high thermal conductivity. These characteristic allow them to perform in extreme conditions of thermo-mechanical loadings [6]. In recent years, there has been a scientific endeavor to solve problem of creep in gears made of conventional materials like metals (aluminum, magnesium …) or ceramics, which operate under high speed rotating. Seok-Chul Hwanga et al. [7] analysis the stress of contact in the pair of rotating gears. They investigated the variation of contact stress for various type of the gear with the different contact positions. Furthermore, they proved that the FEM could be well applied to calculate the gear strength. In another study by Kim et al. [8], the Durability of Plastic gear with glass fiber, reinforced polyamide was examined at different torque levels and rotational speeds. The authors found that as glass fiber reinforced polyamide could potentially improve strength and hardness. Okamoto et al. [9] studied the creep-mechanics of shrink-fit connections for gears and shafts. Their focus was on the study of gears on Interface by using or comparing the results between FEM and experimental approach. Their finding stated that creep is caused by variations in the shear stress distribution on the interfaces along the circumference. Many recent (Stoker et al. [10]) on contact stress evaluation shows that FEM is one of the most prominent methods being used in

stress analysis the stress of gear tooth. Xiang Dai et al. [11] studied the static and dynamic strains of tooth root in gears using finite element simulation. The simulation results of FEM and experimental results are compared. Shuting Li et al. [12] studied the method for exact bending strength and contact strength calculations of a gear at high speed by using finite element method. Their results showed that when gear speed exceeds 10000 rpm, the centrifugal load-deformed thin-walled gear has greater effects on contact pattern of tooth, surface contact stress of tooth and root bending stress. The FGM material has been used to investigate the creep deformations and strength of a various component in industries [13-16]. To the best of our knowledge, the problem of creep deformations in two spur gears has not been investigated in previous literature. The main aim of our work is to present predictions of the creep behavior of the FGM gears by using Norton Law. This helps researchers to gain deep understanding of the behavior of complex deformation, which are engaged with the dynamics of gears. The rest of the paper is arranged as follows. Section 2 discusses the details of the geometry, the description of case studies, and details of the numerical technique. After validation of our results using the experimental and the numerical data, Sec. 3 presents a comprehensive discussion about the obtained results. Finally, engineering advice and criteria are presented in Sec. 4, and Sec. 5 concludes the paper.

2- Creep law, problem formulation and numerical technique

2-1- Geometric data of spur gear to be designed

In present study, spur gear has been designed for transmitting 1.5kW power at 1400 rpm according to Lewis theory [17]. The geometric parameters of spur gear are given as follows:

Table 1: Parameters of gears

Geometric parameter	Values
Module	10 mm
No of teeth	18 - 30
Pressure angle	20°
Addendum	12 mm
Dedendum	13.8 mm
Pitch circle diameter	180 mm

The center of the drive gear considered an origin of the coordinates. Due to the 3D nature of our cases involving two gears rotating, the computational domain is enclosed by two boundaries. The rotation around the axes ox is imposed at the center of drive gear, the rigid wall at the outer side of the two gears. The properties of the different constituents of the FGM (metal, ceramic) used are presented in Table 2.

Table 2: Material properties of the FGM (metal, ceramic) used in simulation [17]

Material	Young's modulus (GPa)	Poisson ratio
Al (metal)	71.5	0.35
Ti (metal)	110	0.35
Cu (metal)	124	0.35
Ni (metal)	214	0.35
TiB (ceramic)	374	0.35

Within ABAQUS, for creep laws other than the power (Norton) law and hyperbolic-sine law, the user subroutine, Creep, should be provided by user to calculate the continuous variation of the material elastic properties between integration points. The subroutine UMAT ABAQUS has been used for variation the Young's modulus in a radial direction of the gear. This subroutine is written in

FORTRAN language. It allows us to create a method to calculate the various variables used by the ABAQUS software. The subroutine was coded so that the Young's modulus is created with appropriate material properties. Due to the variations of the Poisson ratio are much less important than the Young's modulus, it is assumed constant. The Poisson's ratio of Nickel-Steel is is υ=0.291, for TiB2 ceramics it can be υ=0.108. The creep deflection of the functionally graded material gear is calculated by Norton's power law as:

$$\dot{\varepsilon}_e = B\sigma_e^n \quad (1)$$

Where $\dot{\varepsilon}_e$ *and* σ_e are the effective strain rate and stress, respectively. *B* and *n* are material variables illustrating the performance of creep in the FGM gear. The values of creep variables *B* and *n* appearing in the above-mentioned equation depend on the radial variation of reinforcement [18].

$$B(r) = B_0[\frac{V(r)}{V_{ave}}]^{\varphi} \quad (2)$$

$$n(r) = n_0[\frac{V(r)}{V_{ave}}]^{-\varphi} \quad (3)$$

where B_0 and n_0 are the constant coefficients of creep variables *B* and *n* respectively. Also φ is an index of grading. The values of B_0, n_0 and φ are shown in Table 3 as reported in the study of Chen et al. [19].

Table 3: Constant coefficients of the Norton's power law equation [19]

Constant coefficients	value
B_0	2.77×10^{-16}
n_0	3.75
φ	0.7

Figure 1 illustrates the radial variation of Young's modulus for different combinations of the constituents. The FGM material is expressed by the various law that indicated in Table 3, where

$$\alpha = \frac{1}{r}\log(\frac{E_1}{E_2}) \quad (4)$$

where E_1 and E_2 are the metal and ceramic Young's modulus, respectively. In present study ceramic is TiB. Various FGM configurations can be achieved by changing the gradation direction of the constituent materials as:

$$\xi = r \quad (5)$$

The above mentioned gear is analysis for a pair of material such as metal and ceramic. Center of gear and outer side of it has been made by pure metal and TiB (ceramic), respectively (see figure 2). Also, the Young's modulus variation is estimated by four functions as follows: elliptical, power law, exponential and linear. The stress, the strain and the creep deflection are calculated for the rotating FGM gears and the results are shown in different figures.

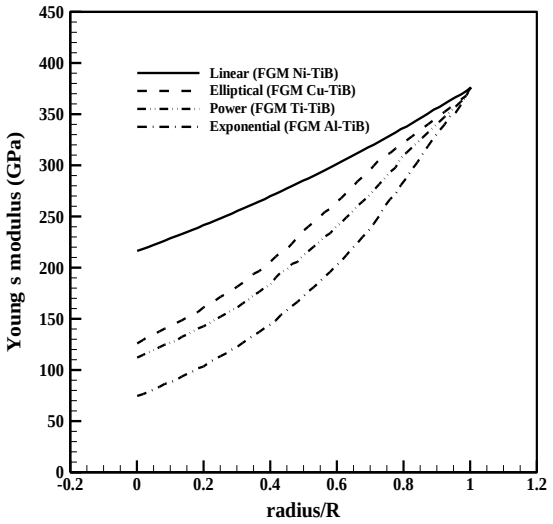

Fig. 1 Variation of Young's modulus in radial direction for different combinations of the constituents.

2-2- Verification of Results

In order to validate results of the current study, the case with Rotating speed of 1300 and teeth No of 25 is considered. Comparison of our data with the experimental visualizations presented by Raptis and Savaidis [20] for the three-dimensional numerical simulation of the two gears creep analysis is illustrated in Fig. 3. The vertical axis refers to the stress at toe of spur gears, and another axis, indicates the number of gear teeth. Figure 3 shows the comparison of the stress at toe of spur gears between the present work and those of Raptis and Savaidis [20]. The maximum relative deviation of the stress for two cases in Fig. 3 is about 6%.

Table 4: FGM Material property functions

Laws	Young's modulus	Density	Poisson ratio
Exponential	$E(\xi)=E_2 e^{\alpha r}$	Const. (average of metal and ceramic)	Const.
Linear	$E(\xi)=E_2(\alpha r)$	Const. (average of metal and ceramic)	Const.
Power	$E(\xi)=E_2 r^2$	Const. (average of metal and ceramic)	Const.
Elliptical	$E^2(\xi)+E_2 r_2^2=\alpha$	Const. (average of metal and ceramic)	Const.

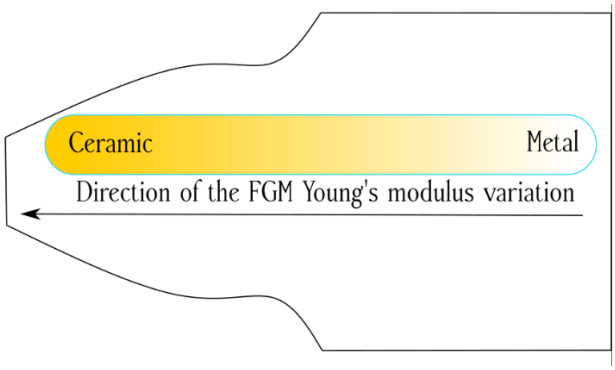

Fig. 2 Direction of the FGM Young's modulus

Table 5: Comparison of maximum von mises stress with the numerical results of Hwang et al [21]

Load type	Maximum stress (MPa) of Hwang et al. [21]	Maximum stress (MPa) of present work
Half load	250.0	230.11
Full load	396.7	400.24

Furthermore, numerical visualizations of Hwang et al. [21] that presented a three-dimensional numerical analysis of the contact stress for a pair of mating gears were compared in Table 5. The maximum von mises stresses obtained by numerically and compared with work of Hwang et al. [21]. Despite a mismatch in conditions and a dearth of timing data, our numerical results show good qualitative agreement with the numerical visualizations of Hwang et al. [21] work.

The contact stress of Hwang et al. [21] work is 250.0 MPa. On the other hand, the stress contour is shown in Fig. 4, and the value of achieved stress is 230.11 MPa. Similarity, in compliance with most experimental works, the high value of

stress is appeared at the contact point and it is spread along the line of contact. As a result, the present work has given a good consistency in comparison with the data obtained by Hwang et al. [21]. Deviation between the stresses for two cases in Fig. 4 is about 7.95 %. The strength calculated on the Hwang et al. [21] work is the most massive value between the values of stress on the contact line. The error might emerge from the various constants applied in the Hwang et al. [21] work.

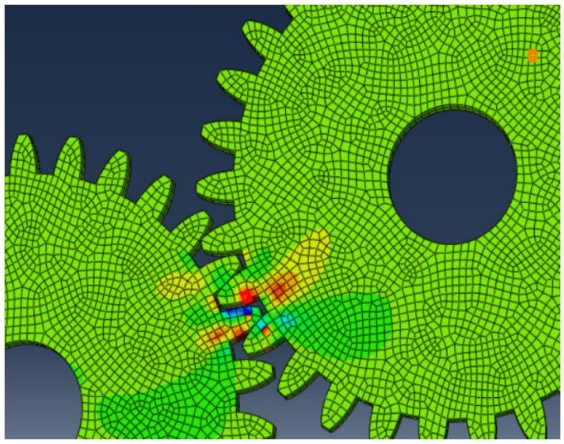

Fig. 4 Stress contour of a mating gear

The utilized numerical mesh consists of the non-structured cells. The grid independence test has been carried out to compute the required number of numerical cells to obtain convergent results. To obtain the grid independent results, simulations have been carried out on three different mesh topologies at Rotating speed of 1300 and teeth No of 25. Three computational meshes were generated with the following details

A(N_z.N_r.N_θ)=40000,
B(N_z.N_r.N_θ)=80000,
C(N_z.N_r.N_θ)=100000.

It is observed that the grids B and C produce almost identical results for the radial creep strain with the relative error less than 0.3%. Hence, the numerical grid B is chosen to have a convergent solution with optimize computational cost. A summary of the output of the grid independence test is shown in Table 6.

Table 6: Grid independence test

Number of mesh	Radial direction creep strain (mm)
A($N_z.N_r.N_\theta$)=40000	0.005478
B($N_z.N_r.N_\theta$)=80000	0.0061254
C($N_z.N_r.N_\theta$)=100000	0.0061025

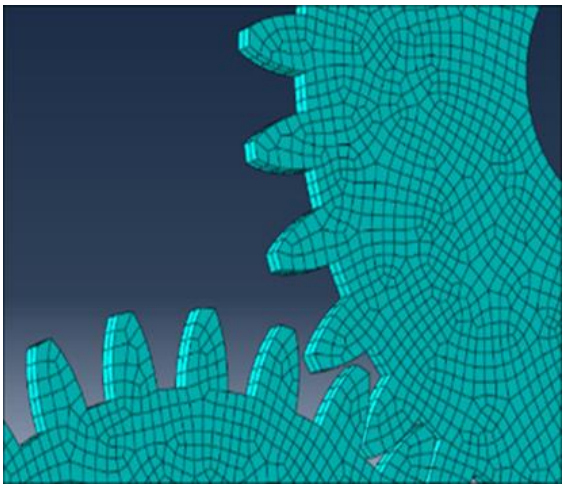

(a) Coarse mesh A

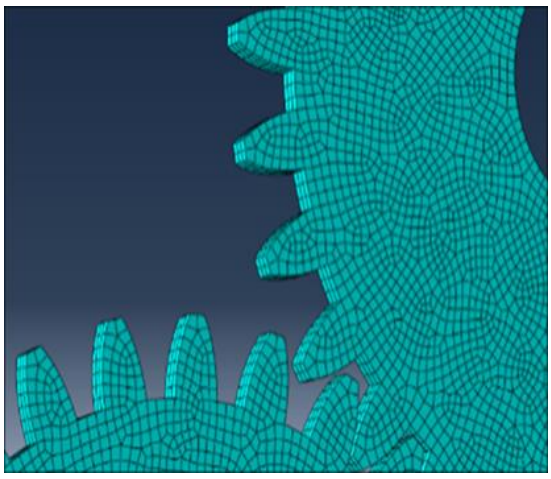

(b) Fine mesh B

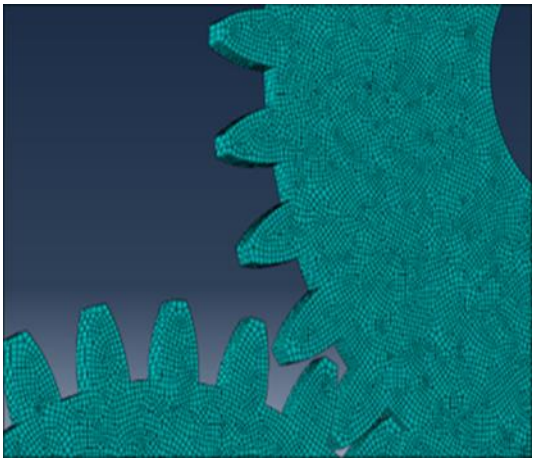

(c) Finest mesh C

Fig. 5 The schematic of the computational domain (a) the coarse mesh A, (b) the fine mesh B, (c) the finest mesh C

The numerical predictions were also analysis with respect to the size of the time-step. So, three different time-steps are considered and the creep strain is computed, yielding the results presented in Table 6. The table proves that the time-step size independent results have been obtained of 10-6.

Table 7: Time step independence test

Time step	Radial direction creep strain (mm)
10^{-3}	0.007145
10^{-6}	0.008452
10^{-9}	0.008325

3- Results and discussion

The above mentioned gears are analysis for a different FGM such as Ni-TiB, Cu-TiB, Ti-TiB and Al-TiB that estimated by the liner, elliptical, power law and exponential equation, respectively. The gears are analysis for uniform face width. Considering the interaction of drive gear with the driven gear, the displacement and stress along the gear involute will be analysis in this section. Radial variation of the gear Young's modulus are linear [23, 24], power law [22], exponential [24, 25] and elliptical equation, which showed in Table 2. These types of functions indicated the different FGM materials.

In our simulation, the rotation speeds are varied as 500, 800, 1100 and 1500 rpm. Variation of stress along the involute of gear is demonstrated in Fig. 7. In Fig. 7, the distribution of stress along the gear involute is influenced by the driven gear rotation speed. For all the cases, the stress is maximum at the gear root portion and creep deflection is maximum at the gear tip portion (see Fig. 6).

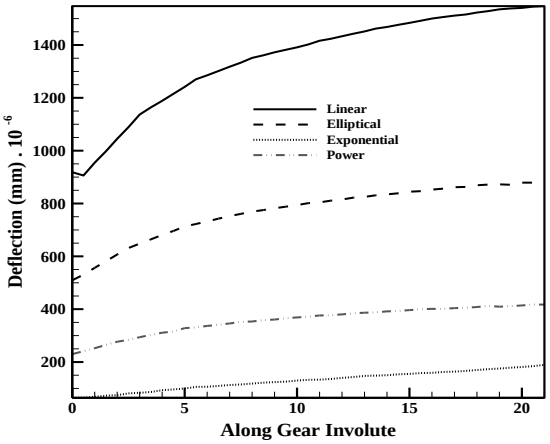

Fig. 6 Variation of deflection

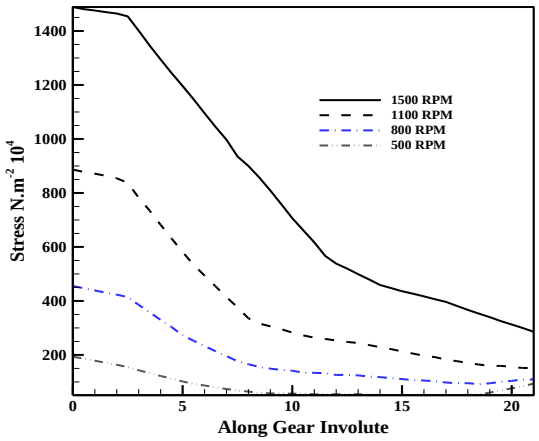

Fig. 7 Variation of stress

It is observed that the creep deflection in the Linear FGM (Ni-TiB) gear increases from 920×10-6 mm to reach a maximum at root portion (see figure 6). With the increase in material gradient in the FGM gears (E2–E1) the creep deflection is changed from curve to linear over the

entire along involute. For all studied FGM materials, the increase is higher in the root portion of the gear than that observed near the tip portion of the gear. The increase observed in the maximum value of creep deflection is about 40.1% as MG (material gradient) in the gear increases from 0 to 25%, as evident from the comparison of Ni-TiB FGM and Al-TiB FGM gears. Furthermore, the creep strains of x, y and radial directions calculated for our cases are listed in Table 8.

Table 8: Comparison between various FGM material creep

Gear notation	Radial direction creep strain (mm)	x direction creep strain (mm)	Y direction creep strain (mm)
Ni-TiB FGM	0.005451	0.0024125	0.0023195
Cu-TiB FGM	0.004785	0.0023145	0.002300
Ti-TiB FGM	0.0041255	0.0019687	0.0018968
Al-TiB FGM	0.0032544	0.0019125	0.0018785

Figure 8 shows the temporal variation of the radial direction creep strain of driven gear for all simulation cases during the 1400 rpm of rotating speed. There are main differences between the radial deflection curves of Ni-TiB and Al-TiB FGM gears. The first one is the more rapid increase of the deflection in the Al-TiB FGM case, and the next one is the appearance high different between them in the deflection curves stemming from the high material gradient.

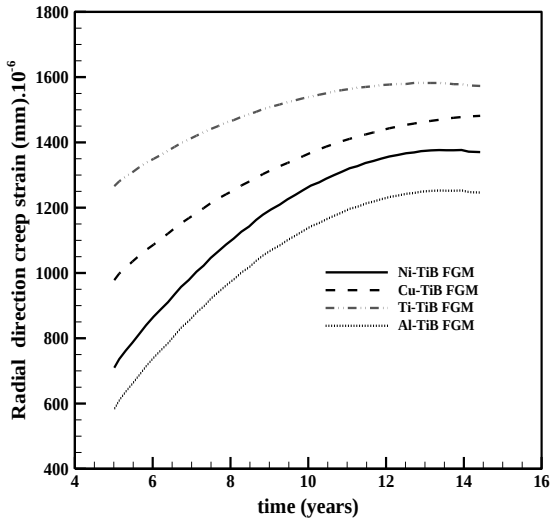

Fig. 8 Variation of creep strain

In applications of the high mechanical and thermal loadings, Al–TiB FGMs gears are suitable. In this FGM, the long life and the minimal lubrication has been expected. Outer side of this FGM consists of ceramic (TiB) as like a glass surface. This smooth surface has a very low friction coefficient causing lower thermal gradient. Properties of ceramic are non-permeability, non-abrasively and smoother surface than metal (Al, Ni, Cu and Ti). In FGM gear, ceramic surfaces are also stronger and harder than metal and due to the surfaces ceramic are non-permeability they are usually frictionless and has a high performance than pure metal gears. As a results that properties increased gear life. However center of FGM gears are made by pure metal, dense center of gears resulting in less oscillation at low speeds operation.

4- Conclusion

In the present work, the functionally graded material gears have been analysis for the strain, the stress and the creep deflection through finite element method. The gear teeth are modelled as three-dimensional geometry in Abaqus 16.2 software. The FGM such as Ni-TiB, Cu-TiB, Ti-TiB and Al-TiB are used in this

study, and its elasticity behavior is varied in radial direction and estimated by various function as follow: exponentially, linearly, power law and elliptically.

Creep deflection of Al–TiB FGM is less than other FGMs due to the high Young's modulus gradient. For all the cases, the stress at the gear root and deflection at the gear tip are maximum value. Finally, the effect of rotating speed on the stress and the strain has been studied and showed that, these parameters are decreased by the increasing of rotation speed.

Nomenclature

FGM	=	Functional Graded Material
R	=	Initial Gear Radius
F	=	Force
p	=	Pressure
t*	=	Life Time
tc	=	Life Time of Creep
u	=	Velocity
ρ	=	Density

Subscripts

c	=	Creep
s	=	Solid

Disclosure Statement

No potential conflict of interest was reported by the author(s).

Acknowledgements

The authors gratefully acknowledge the R&D of the IAU, Isfahan (Khorasgan) and Yadegar-e-Imam Khomeini (RAH), Shahr-e-Rey Branch for the provision of research facilities used in this work.

References

[1] Noda, N., Nakai, S., Tsuji, T. (1998). Thermal stresses in functionally graded materials of particle- reinforced composite. *JSME Int J Series A;*41(2), 178-184.

[2] Raadnui, S. (2019). Spur gear wear analysis as applied for tribological based predictive maintenance diagnostics. Wear, 426, 1748-1760.

[3] Nitin, G., Manish, G., Saini, B. S., Gupta, V. K. (2012). Finite element analysis of creep in a functionally graded rotating disc, Journal of Computer Aided Engineering and Technology, 4(5), 432-444.

[4] Gupta, V. K., Kumar, V., Ray, S. (2009). Modeling creep in a rotating disc with linear and quadratic composition gradients, Engineering Computations, 26(4), 400-421.

[5] Gupta, V. K., Singh, S. B., Chandrawat, H. N., Ray, S. (2004). Steady state creep and material parameters in a rotating disc of Al–SiCP composite, European Journal of Mechanics-A/Solids, 23(2), 335-344.

[6] Gupta, V. K., Chandrawat, H. N., Singh, S. B., Ray, S. (2004). Creep behavior of a rotating functionally graded composite disc operating under thermal gradient. *Metallurgical and Materials Transactions A*, 35(4), 1381-1391.

[7] Seok-Chul Hwanga, Jin-Hwan Lee b, Dong-Hyung Lee c, Seung-Ho Hana, Kwon-Hee Lee, (2013). Contact stress analysis for a pair of mating gears, Mathematical and Computer Modelling, 57, 40-49

[8] Kim, G. H., Lee, J. W., Seo, T. I. (2013). Durability characteristics analysis of plastic worm wheel with glass fiber reinforced polyamide. Materials6(5), 1873-1890.

[9] Okamoto, N., Tanaka, N., Nogami, M. (1996). Finite element and experimental studies of creep at the interface of press fitted gears-shafts connections, Journal of Mechanical Design, 118(4), 568-572.

[10] Stoker, K. C. A (2009). Finite Element Approach To Spur Gear Response And Wear Under Non-Ideal Loading, Doctoral dissertation, University of Florida,

[11] Xiang Daia, Christopher G. Cooley, Robert G. Parkera, (2016). Dynamic tooth root strains and experimental correlations in spur gear pairs, Mechanism and Machine Theory, 101, 60-74.

[12] Shuting Li , (2008). Centrifugal load and its effects on bending strength and contact

strength of a high speed thin-walled spur gear with offset web, Mechanism and Machine Theory, 43(2), 217–239.

[13] Fukui, Y., Yamanaka, N. (1992). Elastic Analysis for Thick Walled Tubes of Functionally Graded Material Subjected to Internal Pressure. JSME Int J Series I, 35(4): 379-385.

[14] Chen, J.J., Tu, S.T., Xuan, F.Z., Wang, Z.D. (2007). Creep analysis for a functionally graded cylinder subjected to internal and external pressure, Journal of Strain Analysis for Engineering Design, 42(2), 69-77.

[15] You, L.H., Ou, H., Zheng, Z.Y, (2007). Creep deformations and stresses in thick-walled cylindrical vessels of functionally graded materials subject to internal pressure, Composite Structure, 78(2), 285-291.

[16] Esmail Abedi, Saeed Daneshmand, Ali Akbar Lotfi Neyestanak, Vahid Monfared (2008). Analysis and modeling of electro discharge machining input parameters of nitinol shape memory alloy by de-ionized water and copper tools, *Journal of Electrochemical Science*, 9(6), 2934-2943.

[17] VB Bhandari, (2008). Design of Machine Elements, 2nd Edition, Tata McGraw-Hill, Publishing Company Limited New Delhi, ISB N0-07-061141-6.

[18] Singh, S. B., Ray, S. (2001). Steady-state creep behavior in an isotropic functionally graded material rotating disc of Al-SiC composite, Metallurgical and Materials Transactions A, 32(7), 1679-1685.

[19] Chen, J. J., Tu, S. T., Xuan, F. Z., Wang, Z. D. (2007). Creep analysis for a functionally graded cylinder subjected to internal and external pressure. The Journal of Strain Analysis for Engineering Design, 42(2), 69-77.

[20] Raptis, K. G., Savaidis, A. A. (2018). Experimental investigation of spur gear strength using photoelasticity, Procedia Structural Integrity, 10, 33-40.

[21] Hwang, S. C., Lee, J. H., Lee, D. H., Han, S. H., Lee, K. H. (2013). Contact stress analysis for a pair of mating gears, Mathematical and Computer Modelling, 57(1-2), 40-49.

[22] Peng, X. L., Li, X. F. (2012). Elastic analysis of rotating functionally graded polar orthotropic disks, Journal of Mechanical Sciences, 60(1), 84-91.

[23] Çallioğlu, H., Bektaş, N. B., Sayer, M. (2011). Stress analysis of functionally graded rotating discs: analytical and numerical solutions, Acta Mechanica Sinica, 27(6), 950-955.

[24] Verma, R.K., Sarda, A. (2016). Analysis of functionally graded material spur gear under static loading condition, Applied Physics Letters, 3, 2349-1108.

[25] M. Heydari Vini, S. Daneshmand, (2019). Effect of Electrically Assisted Accumulative Roll Bonding (EARB) Process on the Mechanical Properties and Microstructure Evolution of AA5083/Al2O3 Composites, Materials Performance and Characterization, 8(1), 594-603.

[26] Mohamad Heydari Vini, Saeed Daneshmand, (2019). Investigation of bonding properties of Al/Cu bimetallic laminates fabricated by the asymmetric roll bonding techniques, Advances in computational design, 4(1), 33-41.